SCIENTIFIC REP⚙RTS

# TXNIP/TRX/NF-κB and MAPK/NF-κB pathways involved in the cardiotoxicity induced by Venenum Bufonis in rats

Qi-rui Bi[1,2,*], Jin-jun Hou[1,*], Peng Qi[1,*], Chun-hua Ma[2], Rui-hong Feng[1], Bing-peng Yan[1,2], Jian-wei Wang[1,2], Xiao-jian Shi[1,2], Yuan-yuan Zheng[1], Wan-ying Wu[1] & De-an Guo[1]

Venenum Bufonis (VB) is a widely used traditional medicine with serious cardiotoxic effects. The inflammatory response has been studied to clarify the mechanism of the cardiotoxicity induced by VB for the first time. In the present study, Sprague Dawley (SD) rats, were administered VB (100, 200, and 400 mg/kg) intragastrically, experienced disturbed ECGs (lowered heart rate and elevated ST-segment), increased levels of serum indicators (creatine kinase (CK), creatine kinase isoenzyme-MB (CK-MB), alanine aminotransferase (ALT), aspartate aminotransferase (AST)) and serum interleukin (IL-6, IL-1β, TNF-α) at 2 h, 4 h, 6 h, 8 h, 24 h, and 48 h, which reflected that an inflammatory response, together with cardiotoxicity, were involved in VB-treated rats. In addition, the elevated serum level of MDA and the down-regulated SOD, CAT, GSH, and GPx levels indicated the appearance of oxidative stress in the VB-treated group. Furthermore, based on the enhanced expression levels of TXNIP, p-NF-κBp65, p-IκBα, p-IKKα, p-IKKβ, p-ERK, p-JNK, and p-P38 and the obvious myocardial degeneration, it is proposed that VB-induced cardiotoxicity may promote an inflammatory response through the TXNIP/TRX/NF-κB and MAPK/NF-κB pathways. The observed inflammatory mechanism induced by VB may provide a theoretical reference for the toxic effects and clinical application of VB.

Venenum Bufonis (VB, Chinese name "Chan Su"), a well-known Traditional Chinese Medicine, is the dried white extract of the auricular and skin glands of *Bufo gargarizans* Cantor or *Bufo melanostictus* Schneider[1]. It has been used traditionally for the treatment of deep-rooted carbuncles and boils, throat swelling and pain, coma, abdominal pain, heart stroke, vomiting, and diarrhea. In addition, it also serves clinically as an anti-cancer, anti-radiation, cardiotonic, diuretic, and anodyne agent[2–5]. The toxicity effects caused by VB have attracted considerable attention, especially the cardiotoxicity, which is a similar manifestation to the effects of digitalis. It is the most severe side effect threatening patients, and may induce bradycardia, atrioventricular conduction blockage, irreversible cardiomyopathy, and even sudden death[6–9].

As is well-known, VB contains a variety of chemical components, including cardiotonic steroids (bufo steroids), indoleamines, fatty acids, polysaccharides, peptides, amino acids, and sterols[10–12]. Unfortunately, the main therapeutic ingredients of VB (bufalin, cinobufotalin, resibufogenin, and cinobufagin) are also the origin of its toxicity[13], and are specific and potent inhibitors of Na^+/K^+ ATPase. To address the cardiotoxicity caused by VB, an increasing number of studies have been reported. *In vitro* studies indicated that the cardio-electrophysiological effects of VB could be due to inhibition of Na^+/K^+-ATPase[14], alteration of calcium transients[15], calcium overload[16] and the redox modification of ryanodine receptors[17]. An *in vivo* metabolomics study demonstrated that the cardiac damage resulting from VB was associated with oxidative stress, mitochondrial dysfunction, and energy metabolism[18]. Although intensive investigations on VB-induced cardiotoxicity have been sustained for decades[19,20], the potential mechanisms of these effects have not been fully elucidated. Considering that Na^+/K^+ ATPase has the functions as a signal transducer or integrator to regulate ROS[21], and the Src/MAPK pathway[22],

[1]Shanghai Research Center for Modernization of Traditional Chinese Medicine, National Engineering Laboratory for TCM Standardization Technology, Shanghai Institute of Materia Medica, Chinese Academy of Sciences, Haike Road 501, Shanghai 201203, China. [2]College of Traditional Chinese Medicine, China Pharmaceutical University, Nanjing 210009, China. *These authors contributed equally to this work. Correspondence and requests for materials should be addressed to W.-Y.W. (email: wanyingwu@simm.ac.cn) or D.-A.G. (email: daguo@simm.ac.cn)
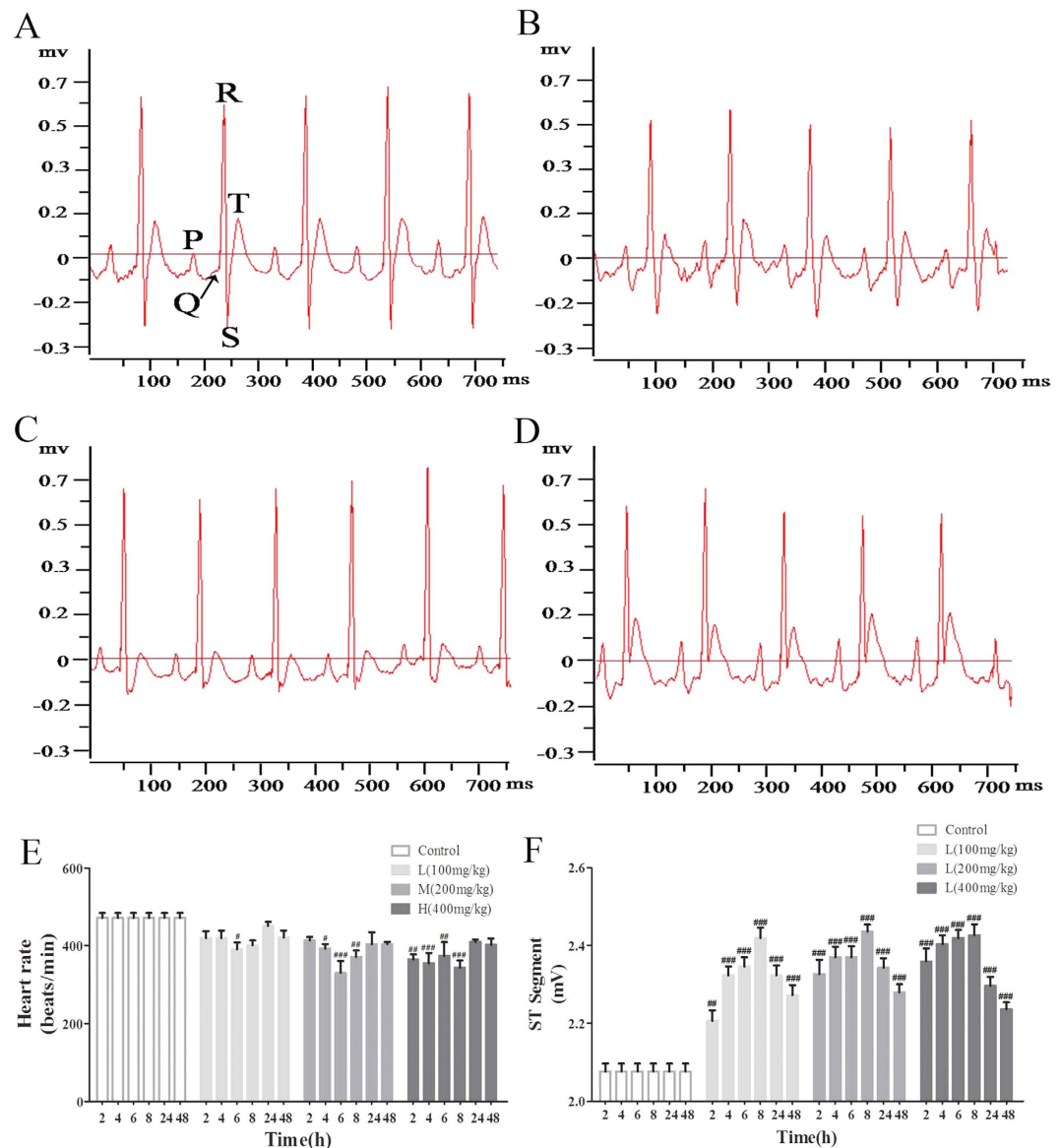
Figure 1. Effects of VB on electrocardiogram (ECG). The representative ECG tracing 4 h after administration of VB (**A–E**). (**A**) Control group; (**B**) 100 mg/kg group; (**C**) 200 mg/kg group; (**D**) 400 mg/kg group; The effects of VB on heart rate (**E**) and the ST-segment derivation (**F**) were statistically analyzed. All values given are the mean $\pm$ SD of eight rats for each group. $^{\#}p < 0.05$, $^{\#\#}p < 0.01$, and $^{\#\#\#}p < 0.001$ vs. control group.

as well as intracellular calcium[23], both the oxidative stress and the inflammatory effects involved in a possible pathology were taken into consideration.

Thioredoxin-interacting protein (TXNIP), the endogenous inhibitor of thioredoxin (TRX), has been linked to oxidative stress and inflammation in a number of diseases, including atherosclerosis[24], myocardial ischemia[25], cancer[26], and the degeneration of the central auditory system[27]. The MAPKs signaling pathway may play an important role in the development of cardiotoxicity[28]. Both TXNIP and MAPK can motivate NF-κB and active downstream genes to further modulate the inflammatory responses which would regulate the pathological state. Thus, the current study focused on the TXNIP/TRX/NF-κB and MAPK/NF-κB pathways to illustrate the inflammatory mechanism of the cardiotoxicity induced by VB, which could be of significance in developing an understanding of the toxic mechanism associated with VB.

Results

Effects of VB on the electrocardiogram (ECG).
The ECGs of rats in the different group were recorded at 2 h, 4 h, 6 h, 8 h, 24 h, and 48 h. Figure 1A–D are representative figures at 4 h of the different groups. Rats in control group did not exhibit any changes in their ECG pattern (Fig. 1A), heart rate (Fig. 1E), and ST-segment derivation (Fig. 1F). Marked disturbances in ECG patterns (Fig. 1B–F) (e.g. elevation of ST-segment and decreased heart rate) were observed in the VB-treated groups.
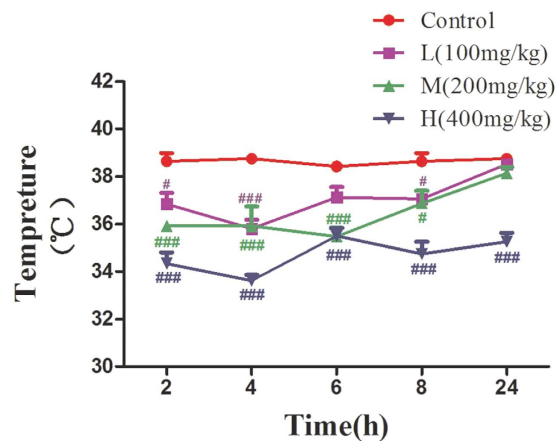
Figure 2. Effects of VB on body temperature. Body temperature was measured after the administration of VB (100 mg/kg, 200 mg/kg, and 400 mg/kg) at 2 h, 4 h, 6 h, 8 h, and 24 h. All values given are the mean ± SD of eight rats for each group. $^{\#}p < 0.05$, $^{\#\#}p < 0.01$, and $^{\#\#\#}p < 0.001$ vs. control group.
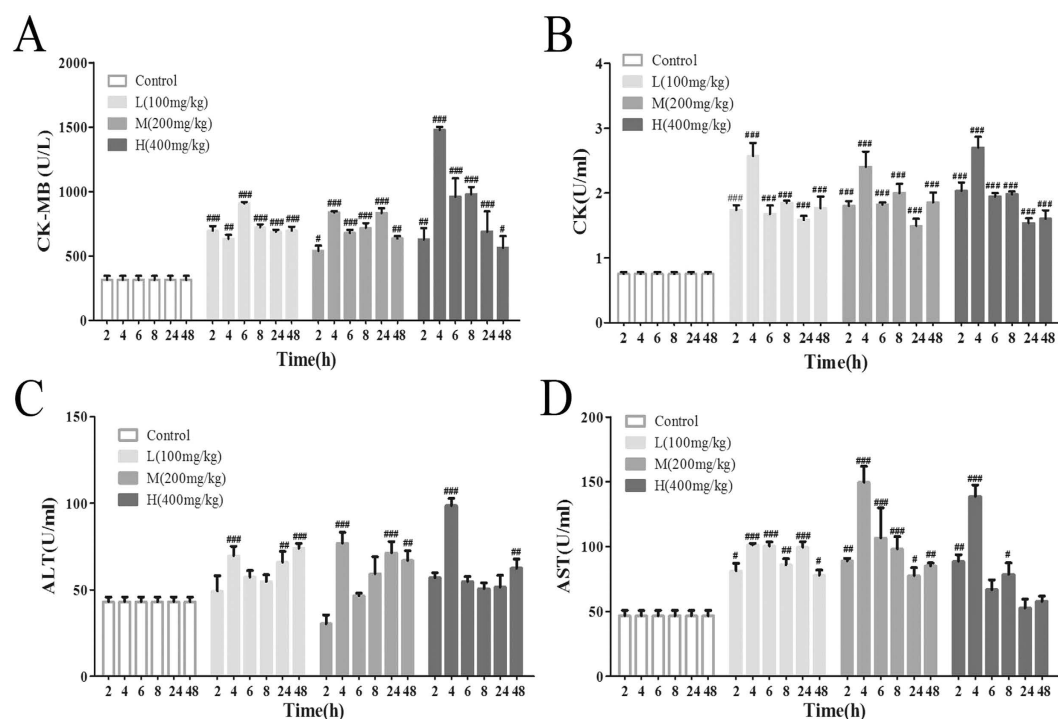

Figure 3. Effects of VB on serum CK-MB (**A**), CK (**B**), ALT (**C**), and AST (**D**). The level of serum CK-MB, CK, AST, and ALT in rats treated with VB (100 mg/kg, 200 mg/kg, and 400 mg/kg) at 2 h, 4 h, 6 h, 8 h, 24 h, and 48 h were test according to the manufacturer's instructions. All values given are the mean ± SD of eight rats for each group. $^{\#}p < 0.05$, $^{\#\#}p < 0.01$, and $^{\#\#\#}p < 0.001$ vs. control group.

Effects of VB on body temperature. Figure 2 shows the anal temperatures recorded during the experiment protocol. As can be seen, the significant reduction of temperature in the VB-treated groups (100 mg/kg, 200 mg/kg, and 400 mg/kg) displayed some degree of dose-dependence compared with the control group examined at 2 h, 4 h, 6 h, 8 h, and 24 h.

Effects of VB on serum CK-MB, CK, AST, and ALT. The effects of VB on serum CK-MB, CK, AST, and ALT level are summarized in Fig. 3. The levels of CK-MB, CK, AST, and ALT in the VB-treated groups (100 mg/kg, 200 mg/kg, and 400 mg/kg) increased to the highest level at 4 h, indicating that the myocardium was damaged quickly after the administration of VB.
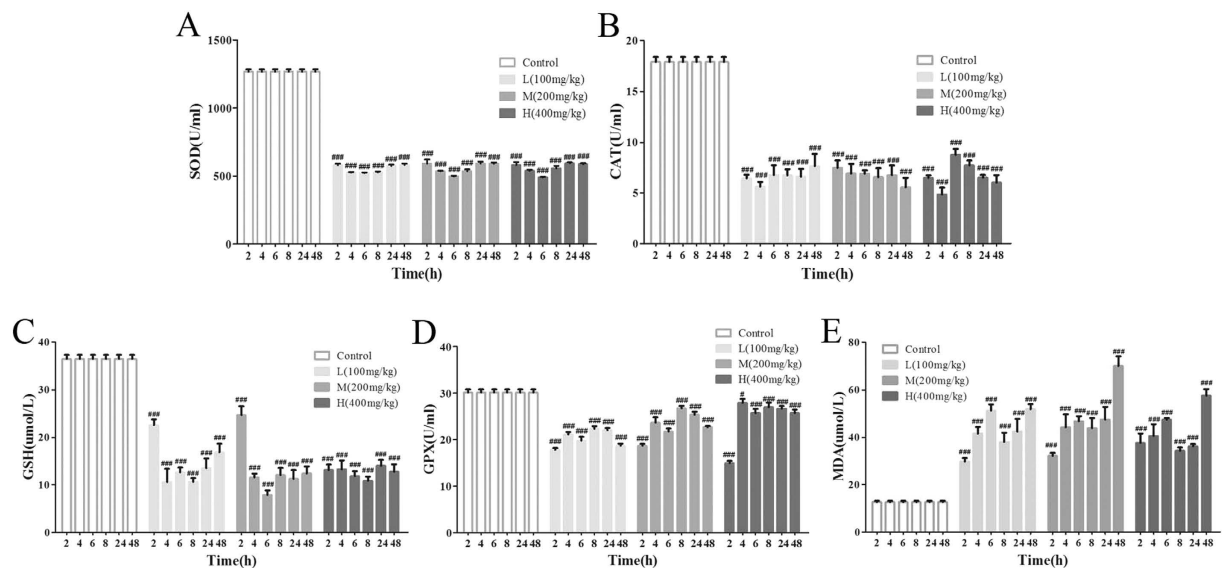
Figure 4. Effects of VB on serum SOD (**A**), CAT (**B**), GSH (**C**), GPx (**D**), and MDA (**E**). Rats were administered with different dosages (100 mg/kg, 200 mg/kg, and 400 mg/kg) of VB. SOD, CAT, GSH, GPx, and MDA were measured at 2 h, 4 h, 6 h, 8 h, 24 h, and 48 h. All values given are the mean $\pm$ SD. $^{\#}p < 0.05$, $^{\#\#}p < 0.01$, and $^{\#\#\#}p < 0.001$ vs. control group (n = 8).
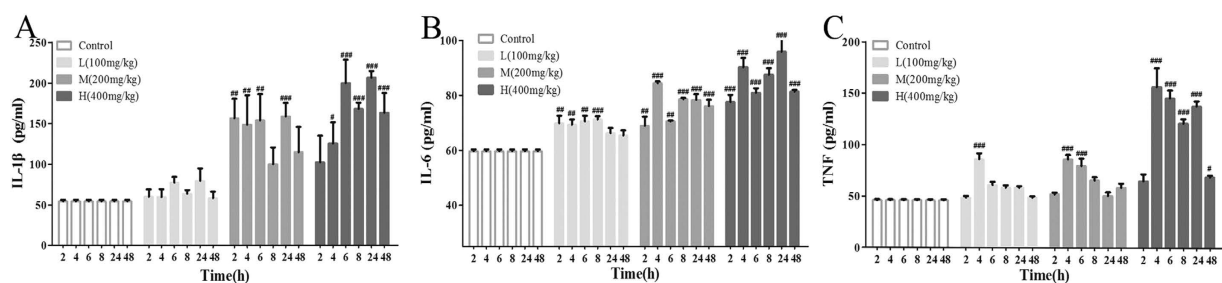

Figure 5. Effects of VB on IL-1β (**A**), IL-6 (**B**), and TNF-α (**C**). The serum pro-inflammatory cytokines IL-1β, IL-6, and TNF-α from different groups at 2 h, 4 h, 6 h, 8 h, 24 h, and 48 h were analyzed by ELISA kits. All values given are the mean $\pm$ SD. $^{\#}p < 0.05$, $^{\#\#}p < 0.01$, and $^{\#\#\#}p < 0.001$ vs. control group (n = 8).

Effects of VB on serum SOD, MDA, CAT, GSH, and GPx.　As shown in Fig. 4, rats treated with VB demonstrated an obvious inhibition of SOD, CAT, GSH, and GPx activity, which indicated the disturbed balance of oxidative stress. In addition, the continuing elevation of MDA, an end product of lipid peroxidation, indicated the involvement of free-radical-induced oxidative injury caused by VB administration.

Effects of VB on cytokine levels.　As shown in Fig. 5, pro-inflammatory cytokines IL-6, IL-1β, and TNF-α in serum showed different degrees of elevation after the various dosages, especially for the middle dosage and the high dosage group at 4 h, 6 h, 8 h, and 24 h in comparison with the control group according to Fig. 5. The observed up-regulation of IL-6, IL-1β, and TNF-α suggested that inflammatory responses had been induced in the VB-treated rats.

Inflammatory mechanism study of the VB-treated rats.　The expressions of TXNIP, TRX, p-NF-κBp65, NF-κBp65, p-IκBα, IκBα, p-IKKα, IKKα, p-IKKβ, and IKKβ, p-ERK, ERK, p-JNK, JNK, p-P38, and P38 in the VB-treated rats (400 mg/kg) were assessed by Western blot analysis. For the TXNIP/TRX/NF-κB pathway, the increase of TXNIP, p-NF-κBp65, p-IKKα, p-IKKβ, and the decrease of TRX in heart tissue, were presented quite clearly. For the MAPK/NF-κB pathways, p-ERK, p-JNK, and p-P38 showed an apparent increase in levels (Fig. 6). Additionally, the enhanced expression of TXNIP, p-NF-κBp65, p-IκBα, p-IKKα, and p-IKKβ in VB(400 mg/kg)-treated rats were clearly observed at 4–48 h by immunohistochemistry (Fig. 7).

Histopathological findings.　To further characterize the cardiotoxicity induced by VB, histopathological examination of heart tissues was conducted. Hearts from the control group animals exhibited regular cell distribution and normal myocardium architecture, while those harvested from the VB-treated groups displayed marked myocardial degeneration, including myofibrillar loss, cytoplasmic vacuolization, inflammatory cell infiltration, congestion, and edema (Fig. 8), which indicated the obvious heart damage.
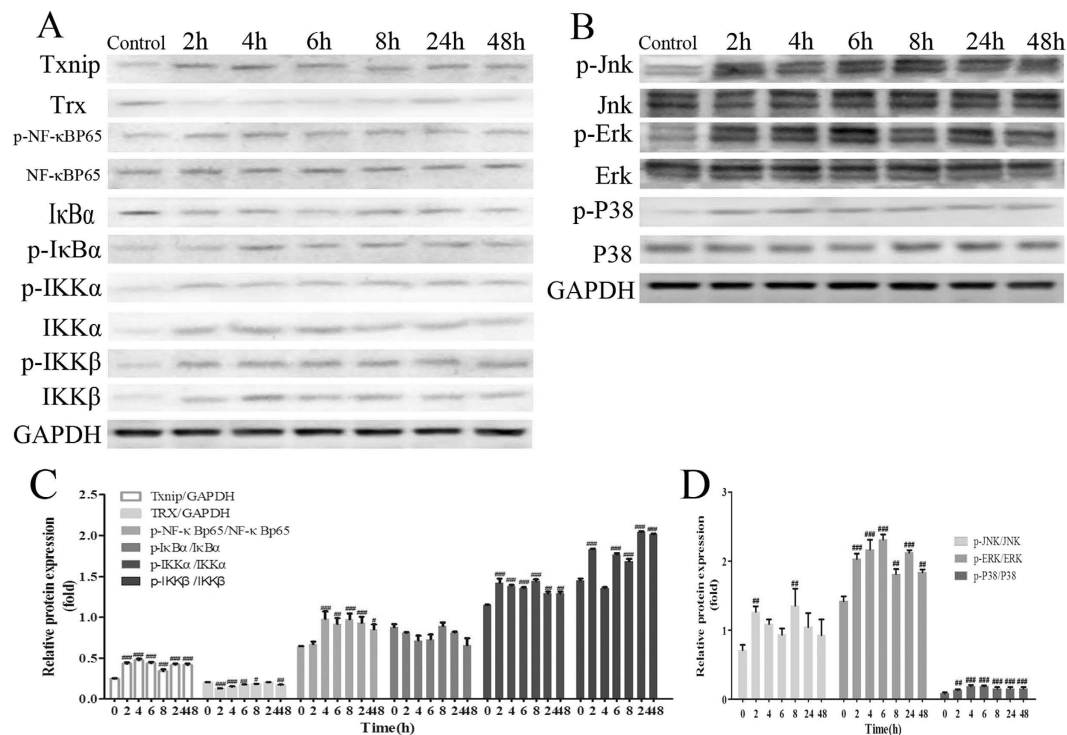
Figure 6. The effect of VB on the TXNIP/NF-κB pathway (**A**) and MAPK/NF-κB pathway (**B**). The expressions of related proteins from the TXNIP/NF-κB pathway and MAPK/NF-κB pathway were studied by Western blot analysis in VB-treated (400 mg/kg) rats. The quantification was performed based on the data of three separated experiments. All values given are the mean ± SD. $^{#}p < 0.05$, $^{##}p < 0.01$, and $^{###}p < 0.001$ vs. control group (n = 3).

Discussion

Due to its various pronounced pharmacological effects, VB is widely used in several Asian countries (e.g. Laos, China, Japan, and India)[29], and has been used clinically for the therapy of a wide range of diseases. However, the toxicity caused by VB limits its clinical application. Although there are an increasing number of reports drawing attention to the adverse cardiovascular effects associated with VB administraion, there is still little known about the mechanism of cardiotoxicity. Here, the TXNIP/TRX/NF-κB and MAPK/NF-κB pathways were intensively studied to investigate the mechanism of cardiotoxicity induced by VB in rats.

The cardiotoxicity effects in VB-treated rats can be observed directly through the readily-observed disturbances in the ECG. A certain degree of myocardial ischemia and arrhythmia can be deduced from the elevated ST-segment and decreased heart rate.

It was reported that body temperature is implicated in the isoprenaline-induced cardiotoxicity in rats[30]. In addition, hyperthermia was shown to be a feature of water-restraint stress-enhanced methamphetamine-induced cardiotoxicity[31]. Myocardial lesions are accompanied by changes in the thermoregulatory capacity of an animal, which can be monitored through alterations in body temperature directly. The data obtained in the present study revealed that different concentrations of VB effectively down-regulated the body temperature of the treated rats, indicating the possible cardiotoxic action of the drug.

Meanwhile, it was confirmed that AST, ALT, CK, and CK-MB, especially for CK-MB, which was released from the damaged myocytes, are the best markers for induced cardiotoxicity because of their tissue specificity[32–34]. The amount of these cellular enzymes present in the blood reflects the changes of serum membrane integrity and/or permeability[35], which indicates certain types of heart damage, such as myocardial infarction, myocarditis, and heart failure. VB administration could lead to damage of the myocardial cell membrane or enhance its permeability, thereby exhibiting the significant elevation in the activities of serum CK-MB, CK, ALT, and AST in the current study. The increases in levels of these enzymes were in agreement with previous investigations[35,36].

The pathogenesis of VB-induced cardiotoxicity is not entirely clear. Accumulating evidence indicates that oxidative stress plays a critical role in the pathogenesis of cardiotoxicity[37,38]. The heart tissue consists of postmitotic cells which intake fatty acids as the preferred substrate for energy supply, making it more susceptible to oxidative stress than other tissues[39]. The myocardium also possesses a set of antioxidant defense systems to prevent free radical invasion and to weaken their damaging effects. Antioxidant enzymes are recognized as the first guard of cell defense that protects the cellular ingredients against damage from oxidative stress. One of the main manifestations of cellular oxidative damage is lipid peroxidation of the myocardial membrane. In addition, as the most abundant non-protein thiol in the cell, GSH is considered to be the major cellular redox buffer. It is implicated in the scavenging of reactive oxygen species and the maintenance of membrane protein thiols. Furthermore, it serves as a substrate for GPx[40]. Briefly, SOD converts superoxide radicals into hydrogen peroxide, which is
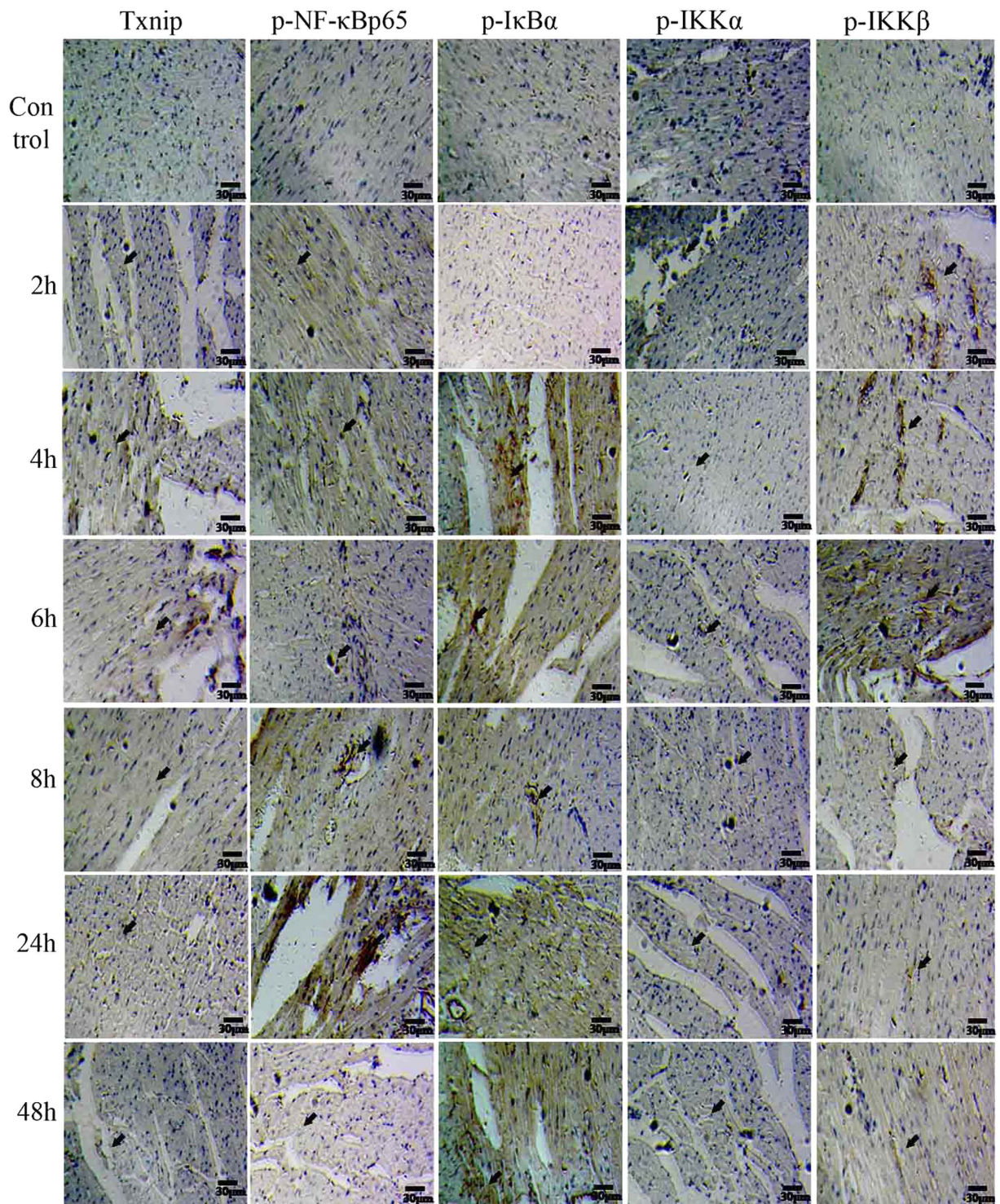
Figure 7. The effect of VB on the TXNIP/NF-κB pathway studied by immunohistochemistry analysis.
The expression of TXNIP, p-NF-κBp65, p-IκBα, p-IKKα, and p-IKKβ of VB (400 mg/kg)-treated rats was investigated by immunohistochemical analysis.

then subsequently catalyzed to water by CAT and GPx. In the present study, oxidative stress was observed in the VB-treated rats, as shown by the decreased antioxidant enzyme CAT and SOD activities, the depleted GSH and GPx levels, and the markedly elevated MDA. Therefore, it is speculated that VB increased the susceptibility of cardiomyocytes to reactive oxygen species, which might be attributed to the reduced activity of SOD and CAT. The level of lipid peroxidation end product, MDA, was markedly increased in the serum of VB-treated rats, which suggested the involvement of free-radical-induced oxidative cell membrane injury[41].
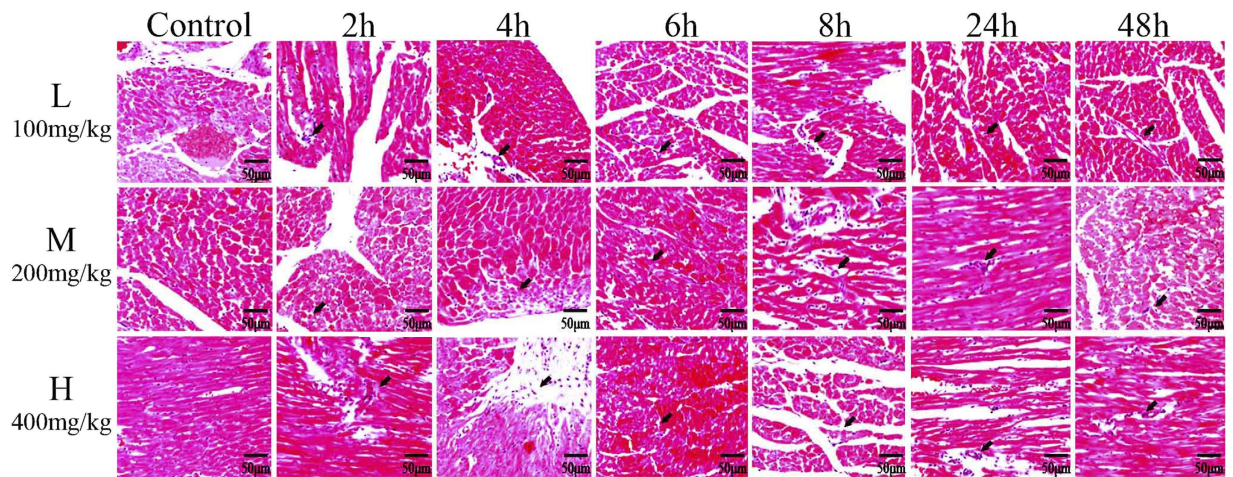
Figure 8. Effects of different VB treatment on myocardium histology. Representative histological changes in heart obtained from rats of different dosage groups (100 mg/kg, 200 mg/kg, and 400 mg/kg) under different times (2 h, 4 h, 6 h, 8 h, 24 h, and 48 h).

Moreover, oxidative stress causes direct deleterious effects, and induces inflammatory responses through activation of the redox sensitive transcription factor NF-κB[42] and the over-production of the pro-inflammatory cytokines IL-6, IL-1β, and TNF-α. As a critical mediator of inflammatory response, NF-κB could also regulate the expression of pro-inflammatory mediators that finally results in fundamental pathological changes in the form of cardiomyopathy, biventricular fibrosis, and transmural myocarditis[43]. In the current study, the serum pro-inflammatory cytokines IL-6, IL-1β, and TNF-α were remarkably up-regulated in the VB-treated group, indicating the potential toxicity of VB. It was assumed that VB might be a potential activator of NF-κB and could enhance the production of downstream inflammatory cytokines.

TXNIP, one of the reactive oxygen species-regulating factors, is related to the maintenance of TRX-mediated redox balance. As a unique protein that reduces thiols, TRX plays a vital role in the regulation of redox balance, cell growth[44], and NF-κB activity. TRX functions as a promoter of NF-κB-dependent transcription by reducing the reactive thiol in the Rel DNA binding domain of the p50/p65 heterodimer[45,46]. NF-κB exists in the cytoplasm in an inactive form through combination with IκB inhibitory proteins. On stimulation, IκB is ubiquitinated and degraded by proteasome revealing the nuclear localization signaling of NF-κB, which promotes the transport of NF-κB from the cytoplasm to the nucleus and accelerates phosphorylation[38]. Interestingly, Hirota *et al.* suggested that over-expression of TRX in the nucleus enhances NF-κB activity, whereas the over-expression in the cytoplasm had the opposite effect, indicating that the upstream proteins of the NF-κB pathway might be suppressed by thiol reduction[47]. It was documented that TXNIP resultant TRX facilitates NF-κB activation and activates the inflammatory response in a model of acute lung injury[48,49]. Furthermore, an implication for the involvement of TXNIP in drug-induced oxidative injury was also reported[50], which might be attributed to its effect on thioredoxin, one of the predominant cellular defense mechanisms against oxidative stress[51], this requires further research. In this study, phosphorylation activated NF-κB p65 was found to be highly expressed in the VB-stimulated rats compared with the control group. Thus, it was proposed that the cardiotoxicity observed in the VB-treated group might be induced by inflammatory effects associated with the TXNIP/TRX/NF-κB pathway activated by oxidative stress.

Moreover, MAPKs, including ERK, JNK, and the p38 signaling pathway, are the key mediators to transform extracellular signals into cellular responses[52]. Diverse studies have shown that reactive oxygen species can also induce or mediate the activation of the MAPK pathways[53]. Activated p38-MAPKs are responsive to stress stimuli and are associated with cell apoptosis, differentiation and autophagy, which plays dual roles in myocardial ischemia-reperfusion injury[54]. Prior work had confirmed that the phosphorylation of p38 MAPK plays a vital role in doxorubicin-induced cardiotoxicity *in vitro*[55]. Specifically, p38 MAPK was demonstrated to be involved in the onset of cardiomyocytes apoptosis in ischemia-reperfusion-injured hearts[56]. Therefore, MAPKs in VB-treated rats were also studied to further explore the mechanism of cardiotoxicity. MAPK activation might act on upstream of the NF-κB pathway, since the inhibitors of MAPK activation have a negative effect on NF-κB activation[57]. The data obtained from the current study showed the increased expression of p-ERK, p-JNK, and p-P38, which was in agreement with previous investigations.

Collectively, the principal finding of this study demonstrated for the first time that the cardiotoxicity induced by VB is involved in inflammation, which might be correlated with TXNIP/TRX/NF-κB and MAPK/NF-κB pathways. Further investigation of VB-induced potential cardiotoxicity might improve the rational use of the drug and promote the development of novel approaches to address the clinical issues during therapy.

Materials and Methods
Main reagents and kits. Venenum Bufonis was purchased from Anhui Province and authenticated by Professor De-an Guo (Shanghai Institute of Materia Medica, Chinese Academy of Sciences). The voucher

specimens were deposited at the Shanghai Research Center for Modernization of Traditional Chinese Medicine, Shanghai Institute of Materia Medica. The major constituents of VB were qualitatively and quantitatively analyzed, as shown in the supplementary information (see supplementary Fig. S1 and supplementary Table S1 online). TNF-α, IL-6, and IL-1β enzyme-linked immunosorbent assay (ELISA) kits were supplied by Nanjing KeyGEN Biotech. Co., Ltd. (Nanjing, China). CK-MB, CK, AST, ALT, MDA, SOD, CAT, GSH, and GPx kits were purchased from Jiancheng Bioengineering Institute (Nanjing, China). Primary antibodies against TXNIP, TRX, p-NF-κBp65, NF-κBp65, p-IκBα, IκBα, p-IKKα, IKKα, p-IKKβ, and IKKβ, p-ERK, ERK, p-JNK, JNK, p-P38, and P38 antibodies were produced by Cell Signaling Technology (Danvers, Massachusetts, USA).

All other chemicals and reagents used in the studies were of analytical grade and were purchased from approved organizations.

Animals. Sprague Dawley (SD) rats (84 male and 84 female), weighing 180–220 g, were acquired from the Comparative Medicine Centre of Yangzhou University. They were housed in an animal center under standard laboratory conditions with a 12 h light/12 h dark cycle environment at 22–24 °C, humidity of 40–70%, and had free access to standard water and food pellets. All experimental procedures were carried out in strict accordance with the NIH Guidelines for the Care and Use of Laboratory Animals, and all protocols were approved by the Institutional Animal Care and Use Committee of the Shanghai Institute of Materia Medica. All surgery was performed under sodium pentobarbital anesthesia and all efforts were spared to ensure minimal animal suffering.

Experimental protocols. According to the previous studies, the dose of VB administered to rats (Wistar rats and Sprague-Dawley rats) is between 100–500 mg/kg[58–60]. The previous acute toxicity study indicated that the LD$_{50}$ was 786–800 mg/kg based on an ICR mouse model, which is equivalent to 550–560 mg/kg for rats in our laboratory. Dong et al. used 10-week old rats (240–300 g) administered intragastrically with a high dose of VB (500 mg/kg) because of the close positive relationship between toxicity tolerance and weight[58]. In this study, considering the weight variation between male and female rats, the use of 6-week old rats (weighing 180–220 g) was adopted. To minimize the occurrence of morbidity, the 400 mg/kg high dose was administered intragastrically. VB was ground into a 60-mesh powder and suspended in 0.5% carboxymethyl cellulose sodium salt (CMC-Na) aqueous solution.

The rats were randomly divided into seven groups (n = 24), each comprised of half males and half females as follows: control group, 2 h group, 4 h group, 6 h group, 8 h group, 24 h group, and 48 h group. Apart from the control group (n = 8) which were administered with 0.5% CMC-Na aqueous solution, each group consisted of three subgroups (n = 8) at the different doses of VB (100 mg/kg), VB (200 mg/kg), and VB (400 mg/kg).

Recording of the electrocardiogram (ECG). Rats were anaesthetized with sodium pentobarbital by intraperitoneal injection at 2 h, 4 h, 6 h, 8 h, 24 h, and 48 h after drug administration, then the ECG were recorded using the BL-420 S Biologic Function Experiment system (Chengdu, China), and the heart rate and ST-segment derivation were statistically analyzed.

Effects of VB on body temperature. Anal temperatures of each group were recorded by electronic thermometer T15SL (Guangzhou Genial Technology Co., Ltd., Guangzhou, China) prior to the anesthesitic procedure.

Sample preparation. After the rats were sacrificed, blood samples were collected from the carotid artery and centrifuged at 5000 rpm for 15 min. The supernatant were collected and set aside at −80 °C for analysis of biochemical parameters. In addition, hearts were harvested and stored at −80 °C waiting for Western blot analysis, immunohistochemical analysis, and histological studies.

Measurement of the CK-MB, CK, AST, and ALT contents in serum. CK-MB, CK, AST, and ALT are important serum markers to assess myocardial function. Their activities were detected using the applicable ELISA kits according to the manufacturer's instructions.

Measurement of the SOD, CAT, GSH, GPx, and MDA contents in serum. The activity of SOD, GSH, GPx, and CAT, as well as the content of MDA, were determined using the applicable ELISA kits on the basis of the manufacturer's instructions.

Measurement of the cytokine content in serum. The concentrations of IL-6, IL-1β, and TNF-α in serum were analyzed by the applicable ELISA kits according to the manufacturer's instructions.

Western blot analysis. Myocardial tissues were minced and homogenized in ice-cold RIPA lysis buffer. Dissolved proteins were harvested and centrifuged at 12000 rpm for 5 min at 4 °C to remove the debris. The concentration of total protein was detected with the bicinchoninic acid (BCA) protein assay reagent. Equal amounts of protein were mixed with five-times loading dye (Laemmli Sample Buffer) and 2-mercaptoethanol, followed by heating at 95 °C for 5 min, they were then loaded onto SDS-polyacrylamide gel electrophoresis and transferred onto the polyvinylidene difluoride membrane. A blocking solution (5% non-fat milk in PBS) was used to incubate the sheets overnight at 4 °C using specific antibodies against TXNIP, TRX, p-NF-κBp65, NF-κBp65, p-IκBα, IκBα, p-IKKα, IKKα, p-IKKβ, IKKβ, p-ERK, ERK, p-JNK, JNK, p-P38, P38, and GAPDH. After washing with TBST three times, the bands were incubated for 1 h at room temperature with the corresponding secondary antibodies. Enhanced chemiluminescence detection (ECL) reagents and a gel imaging system (Tanon Science &

Technology Co., Ltd., Shanghai, China) were used to visualize the membranes. Densitometric scanning of band intensities were performed by Quantity one (Bio-Rad, California, USA).

Immunohistochemical analysis. Myocardial tissues were fixed in 10% (V/V) neutral buffered formalin for 48 h, embedded in paraffin wax, and cut into 4 μm thick slices. The paraffin sections were baked for 1 h in the oven, deparaffinized in xylene, rehydrated with graded ethanol solutions, microwaved in sodium citrate buffer, cooled to room temperature naturally and incubated in 3% hydrogen peroxide. Each section was blocked with 3% BSA at room temperature. After removing the blocking solution, sections were incubated with primary antibody overnight at 4 °C, The membrane was washed three times with TBST containing Tween 20, and incubated with horseradish peroxidase-conjugated secondary anti-rabbit antibodies for 1.5 h. After that, the samples were stained with DAB and then re-stained with hematoxylin. After dehydration and drying, the sections were mounted with neutral gum.

Histological studies. Heart tissue sections were deparaffinized in xylene, processed with a graded ethanol series, and then stained with hematoxylin-Eosin (HE) solution for examination of the histopathology.

Statistical analysis. All data were expressed as means ± standard deviation (SD). One-way analysis of variance (ANOVA) with the Tukey multiple comparison test was performed to evaluate the differences between groups. Figures were considered as statistically significant when p values < 0.05. Calculations were made using GraphPad Prism 5.0 (Graphpad, San Diego, CA, USA).

References

1. Kim, J. S. *et al.* Antitumor effect of skin of Venenum Bufonis in a NCI-H460 tumor regression model. *J Acupunct Meridian Stud.* **3,** 181–187 (2010).
2. Chen, K. K. & Kovarikove, A. Pharmacology and toxicology of toad venom. *J Pharm Sci.* **56,** 1535–1541 (1967).
3. Dong, W. B., Wu, B. L. & Zhu, M. H. Clinical efficacy and functional characteristics of toad venom preparation. *Chin Med Pharm J.* **2,** 26–27 (2003).
4. Shimada, K. *et al.* Studies on cardiotonic steroids from the skin of Japanese toad. *Chem Pharm Bull.* **25,** 714–730 (1977).
5. Chinese Pharmacopoeia Committee. *Pharmacopoeia of the People's Republic of China.* (Chinese Pharmacopoeia Committee, 2010).
6. Kostakis, C. & Byard, R. W. Sudden death associated with intravenous injection of toad extract. *Forensic Sci Int.* **188,** 1–5 (2009).
7. Yoo, W. S. *et al.* Toxicity studies on secretion Bufonis: a traditional supplement in Asia. *J Acupunct Meridian Stud.* **2,** 159–164 (2009).
8. Gowda, R., Cohen, R. & Khan, I. Toad venom poisoning: resemblance to digoxin toxicity and therapeutic implications. *Heart.* **89,** e14–e14 (2003).
9. Kwan, T., Paiusco, A. & Kohl, L. Digitalis toxicity caused by toad venom. *Chest.* **102,** 949–950 (1992).
10. Ye, M., Guo, H., Han, J. & Guo, D. Simultaneous determination of cytotoxic bufadienolides in the Chinese medicine ChanSu by high-performance liquid chromatography coupled with photodiode array and mass spectrometry detections. *J Chromatogr B: Anal Technol Biomed Life Sci.* **838,** 86–95 (2006).
11. Luo, X. P. *et al.* Microemulsion electrokinetic chromatographic determination of bufadienolides in toad venom and in traditional Chinese medicine. *Anal Bioanal Chem.* **84,** 1254–1258 (2006).
12. Hu, Y. M. *et al.* Comprehensive chemical analysis of Venenum Bufonis by using liquid chromatography/electrospray ionization tandem mass spectrometry. *J Pharm Biomed Anal.* **56,** 210–220 (2011).
13. Steyn, P. S. & van Heerden, F. R. Bufadienolides of plant and animal origin. *Nat Prod Rep.* **15,** 397–413 (1998).
14. Abdel-Rahman, M. A., Ahmed, S. H. & Nabil, Z. I. *In vitro* cardiotoxicity and mechanism of action of the Egyptian green toad *Bufo viridis* skin secretions. *Toxicol in vitro.* **24,** 480–485 (2010).
15. Bick, R. J., Poindexter, B. J., Sweney, R. R. & Dasgupta, A. Effects of Chan Su, a traditional Chinese medicine, on the calcium transients of isolated cardiomyocytes: Cardiotoxicity due to more than Na, K-ATPase blocking. *Life Sci.* **72,** 699–709 (2002).
16. Ruch, S. R., Nishio, M. & Wasserstrom, J. A. Effect of cardiac glycosides on action potential characteristics and contractility in cat ventricular myocytes: role of calcium overload. *J Pharmacol Exp Ther.* **307,** 419–428 (2003).
17. Ho, G. T. *et al.* Arrhythmogenic adverse effects of cardiac glycosides are mediated by redox modification of ryanodine receptors. *J Physiol.* **589,** 4697–4708 (2011).
18. Dong, G. *et al.* Study of the cardiotoxicity of Venenum Bufonis in rats using an 1 H NMR-based metabolomics approach. *PLoS One.* **10,** 1–22 (2015).
19. Ma, H. *et al.* Protective effect of taurine on cardiotoxicity of the bufadienolides derived from toad (*Bufo bufo gargarizans* Canto) venom in guinea-pigs *in vivo* and *in vitro*. *Toxicol Mech Methods.* **22,** 1–8 (2012).
20. Ma, H. *et al.* The novel antidote Bezoar Bovis prevents the cardiotoxicity of toad (*Bufo bufo gargarizans* Canto) venom in mice. *Exp Toxicol Pathol.* **64,** 417–423 (2012).
21. Yan, Y. L. *et al.* Involvement of reactive oxygen species in a feed-forward mechanism of Na/K-ATPase-mediated signaling transduction. *J Biol Chem.* **22,** 34249–34258 (2013).
22. Wang, Z. *et al.* Cardiac glycosides inhibit p53 synthesis by a mechanism relieved by Src or MAPK inhibition. *Cancer Res.* **69,** 6556–6564 (2009).
23. Balasubramaniam, S. L. *et al.* Sodium-calcium exchanger 1 regulates epithelial cell migration via calcium-dependent extracellular signal-regulated kinase signaling. *J Biol Chem.* **290,** 12463–12473 (2015).
24. Berk, B. C. Novel approaches to treat oxidative stress and cardiovascular diseases. *Trans. Am. Clin. Climatol. Assoc.* **118,** 209–214 (2007).
25. Yoshioka, J. *et al.* Deletion of thioredoxin-interacting protein in mice impairs mitochondrial function but protects the myocardium from ischemia-reperfusion injury. *J. Clin. Invest.* **122,** 267–279 (2012).
26. Li, W. *et al.* Hyperglycemia regulates TXNIP/TRX/ROS axis via p38 MAPK and ERK pathways in pancreatic cancer. *Curr Cancer Drug Targets.* **14,** 348–56 (2014).
27. Sun, H. Y. *et al.* Age-related changes in mitochondrial antioxidant enzyme Trx2 and TXNIP–Trx2–ASK1 signal pathways in the auditory cortex of a mimetic aging rat model: changes to Trx2 in the auditory cortex. *FEBS J.* **282,** 2758–2774 (2015).
28. Shah, A. *et al.* Thioredoxin-interacting protein mediates high glucose-induced reactive oxygen species (ROS) generation by mitochondria and the NADPH oxidase, Nox4, in mesangial cells. *J. Biol. Chem.* **288,** 6835–6848 (2013).
29. Ashok, G., Sakunthala, S. R. & Rajasekaran, D. An interesting case of cardiotoxicity due to bufotoxin (toad toxin). *J Assoc Physicians India.* **59,** 737–738 (2011).
30. Harri, M. N. Effect of body temperature on cardiotoxicity of isoprenaline in rats. *Acta Pharmacol Toxicol (Copenh).* **39,** 214–224 (1976).

31. Tomita, M. L. *et al.* Water-restraint stress enhances methamphetamine induced cardiotoxicity. *Chem Biol Interact.* **190,** 54–61 (2011).
32. Singal, P. K., Deally, C. M. & Weinberg, L. E. Subcellular effects of adriamycin in the heart: a concise review. *J Mol Cell Cardiol.* **19,** 817–828 (1987).
33. Khan, G. *et al.* Cardioprotective effect of green tea extract on doxorubicin-induced cardiotoxicity in rats. *Acta Pol Pharm.* **71,** 861–868 (2014).
34. Amran, A. Z., Jantan, I., Dianita, R. & Buang, F. Protective effects of the standardized extract of Zingiber officinale on myocardium against isoproterenol-induced biochemical and histopathological alterations in rats. *Pharm Biol.* **53,** 1795–1802 (2015).
35. Koti, B. C. *et al.* Cardioprotective effect of Vedic Guard against doxorubicin-induced cardiotoxicity in rats: A biochemical, electrocardiographic, and histopathological study. *Pharmacogn Mag.* **9,** 176–181 (2013).
36. Ibrahim, M. A. *et al.* Angiotensin-converting enzyme inhibition and angiotensin AT (1)-receptor antagonism equally improve doxorubicin induced cardiotoxicity and nephrotoxicity. *Pharmacol. Res.* **60,** 373–381 (2009).
37. Minotti, G. *et al.* Anthracyclines: molecular advances and pharmacologic developments in antitumor activity and cardiotoxicity. *Pharmacol. Rev.* **56,** 185–229 (2004).
38. Mantawy, E. M. *et al.* Chrysin alleviates acute doxorubicin cardiotoxicity in rats via suppression of oxidative stress, inflammation and apoptosis. *Eur J Pharmacol.* **728,** 107–118 (2014).
39. Sohal, R. S. & Weindruch, R. Oxidative stress, caloric restriction and aging. *Science.* **273,** 59–63 (1996).
40. Townsend, D. M., Tew, K. D. & Tapiero, H. The importance of glutathione in human disease. *Biomed Pharmacother.* **57,** 144–155 (2003).
41. Yahya, M. D., Pinnas, J. L., Meinke, G. C. & Lung, C. C. Antibodies against malondialdehyde (MDA) in MRL/lpr/lpr mice: evidence for an autoimmune mechanism involving lipid peroxidation. *J. Autoimmun.* **9,** 3–9 (2015).
42. Rahman, I. Oxidative stress, transcription factors and chromatin remodelling in lung inflammation. *Biochem. Pharmacol.* **64,** 935–942 (2002).
43. Bozkunt, B. *et al.* Pathophysiologically relevant concentration of tumor necrosis factor-alpha promote progressive left ventricular dysfunction and remodelling in rats. *Circulation.* **97,** 1382–1391 (1998).
44. Schulze, P. C. *et al.* Vitamin D-3-upregulated protein-1 (VDUP-1) regulates redox-dependent vascular smooth muscle cell proliferation through interaction with thioredoxin. *Circ Res.* **91,** 689–695 (2002).
45. Harper, R. *et al.* Activation of nuclear factor-κB transcriptional activity in airway epithelial cells by thioredoxin but not by N-acetylcysteine and glutathione. *Am J Respir Cell Mol. Biol.* **25,** 178–185 (2001).
46. Matthews, J. R. *et al.* Thioredoxin regulates the DNA binding activity of NF-κB by reduction of a disulphide bond involving cysteine 62. *Nucleic Acids Res.* **20,** 3821–3830 (1992).
47. Hirota, K. *et al.* Distinct roles of thioredoxin in the cytoplasm and in the nucleus. *J. Biol. Chem.* **274,** 27891–27897 (1999).
48. Kelleher, Z. T. *et al.* NOS2 regulation of LPS-induced airway inflammation via S-nitrosylation of NF-κB p65. *Am J Physiol Lung Cell Mol Physiol.* **301,** 327–333 (2011).
49. Marshall, H. E. *et al.* Protection from lipopolysaccharide-induced lung injury by augmentation of airway S-nitrosothiols. *Am J Respir Crit Care Med.* **180,** 11–18 (2009).
50. Gao, K. *et al.* A novel TXNIP-based mechanism for Cx43-mediated regulation of oxidative drug injury. *J Cell Mol Med.* **19,** 2469–2480 (2015).
51. Schulze, P. C. *et al.* Hyperglycemia promotes oxidative stress through inhibition of thioredoxin function by thioredoxin-interacting protein. *J Biol Chem.* **279,** 30369–30374 (2004).
52. Li, W. *et al.* Hyperglycemia regulates TXNIP/TRX/ROS axis via p38 MAPK and ERK pathways in pancreatic cancer. *Curr Cancer Drug Targets.* **14,** 348–356 (2014).
53. McCubrey, J. A., Lahair, M. M. & Franklin, R. A. Reactive oxygen species-induced activation of the MAP kinase signaling pathways. *Antioxid Redox Signal.* **8,** 1775–1789 (2006).
54. Kovalska, M. *et al.* Intracellular signaling MAPK Pathway after cerebral ischemia-reperfusion injury. *Neurochem Res.* **37,** 1568–1577 (2015).
55. Guo, R. *et al.* Hydrogen sulfide attenuates doxorubicin-induced cardiotoxicity by inhibition of the p38 MAPK pathway in H9c2 cells. *Int J Mol Med.* **31,** 644–650 (2013).
56. Bogoyevitch, M. A. *et al.* Stimulation of the stress-activated mitogen-activated protein kinase subfamilies in perfused heart. p38/RK mitogen-activated protein kinases and c-Jun N-terminal kinases are activated by ischemia/reperfusion. *Circ Res* **79,** 162–173 (1996).
57. Jang, S. I. *et al.* Tanshinone IIA inhibits LPS-induced NF-κB activation in RAW 264.7 cells: possible involvement of the NIK-IKK, ERK1/2, p38 and JNK pathways. *European Journal of Pharmacology.* **542,** 1–7 (2006).
58. Dong, G. *et al.* Study of the cardiotoxicity of Venenum Bufonis in rats using an ^{1}H NMR-based metabolomics approach. *Plos one.* **10,** e0119515 (2015).
59. Xia, X. L., Jin, H. Z., Yan, S. K. & Zhang, W. D. Analysis of the bioactive constituents of ChanSu in rat plasma by high performance liquid chromatography with mass spectrometric detection. *J Pharmaceut Biomed.* **53,** 646–654 (2010).
60. Liang, Y. *et al.* Simultaneous determination and pharmacokinetics of five bufadienolides in rat plasma after oral administration of Chansu extract by SPE-HPLC method. *J Pharmaceut Biomed.* **46,** 442–448 (2008).

Acknowledgements

Author Contributions

J.-J.H., P.Q. and Q.-R.B. participated in the study design, performing of experiments and drafting of manuscript. C.-H.M., R.-H.F., B.-P.Y., J.-W.W., X.-J.S. and Y.-Y.Z. performed the animal experiments. W.-Y.W. and D.-A.G. were involved in the design of the study and the revision of the manuscript. All authors read and approved the final version of the manuscript.

Additional Information

Supplementary information accompanies this paper at http://www.nature.com/srep

Competing financial interests: The authors declare no competing financial interests.